Apical membrane maturation and cellular rosette formation during morphogenesis of the zebrafish lateral line

David Hava[1,*], Ulrike Forster[1,*], Miho Matsuda[2], Shuang Cui[3], Brian A. Link[3], Jenny Eichhorst[4], Burkhard Wiesner[4], Ajay Chitnis[2] and Salim Abdelilah-Seyfried[1,‡]

[1]Max Delbrück Center (MDC) for Molecular Medicine, D-13125 Berlin, Germany
[2]Unit on Vertebrate Neural Development, Laboratory of Molecular Genetics, NIH/NICHD, Bethesda, MD 20892, USA
[3]Medical College of Wisconsin, Department of Cell Biology, Neurobiology and Anatomy, Milwaukee, WI 53226, USA
[4]Leibniz Institute for Molecular Pharmacology (FMP), D-13125 Berlin, Germany

*These authors contributed equally to this work
‡Author for correspondence (e-mail: salim@mdc-berlin.de)

Accepted 14 November 2008
Journal of Cell Science 122, 687-695 Published by The Company of Biologists 2009
doi:10.1242/jcs.032102

Summary

Tissue morphogenesis and cell sorting are major forces during organ development. Here, we characterize the process of tissue morphogenesis within the zebrafish lateral line primordium, a migratory sheet of cells that gives rise to the neuromasts of the posterior lateral line organ. We find that cells within this epithelial tissue constrict actin-rich membranes and enrich apical junction proteins at apical focal points. The coordinated apical membrane constriction in single Delta D-positive hair cell progenitors and in their neighbouring prospective support cells generates cellular rosettes. Live imaging reveals that cellular rosettes subsequently separate from each other and give rise to individual neuromasts. Genetic analysis uncovers an involvement of Lethal giant larvae proteins in the maturation of apical junction belts during cellular rosette formation. Our findings suggest that apical constriction of cell membranes spatially confines regions of strong cell-cell adhesion and restricts the number of tightly interconnected cells into cellular rosettes, which ensures the correct deposition of neuromasts during morphogenesis of the posterior lateral line organ.

Key words: Lethal giant larvae 2, Cell polarity, Lateral line organ, Protein kinase Cι, Heart and soul, Adhesion

Supplementary material available online at
http://jcs.biologists.org/cgi/content/full/122/5/687/DC1

Introduction

One of the fundamental problems in developmental biology is understanding how the behaviour of single cells affects global tissue and organ morphogenesis. The development of the zebrafish posterior lateral line primordium (PLLP) provides an excellent system for the study of dynamic single cell behaviours that contribute to higher order tissue organization (Ghysen and Dambly-Chaudière, 2007). The lateral line is a sensory system found in fish and amphibians that is dedicated to the detection of water movements. These movements are registered by specialized sense organs, the neuromasts, which consist of a central mechanosensory hair cell bundle and surrounding support cells. The lateral line system itself can be divided into two parts: an anterior one, which comprises the neuromasts of the head; and a posterior one, which comprises the neuromasts of the body and tail. Most of the research in the field has focused on the development of the posterior lateral line (PLL), owing to its stereotypy and to its amenity to experimental manipulation. In zebrafish, the PLL derives from the PLLP, which is a small cohesive tissue of ~100 cells. After delaminating from its origin (an epidermal placode just posterior of the otic vesicle) at ~18-20 hours post-fertilization (hpf) (reviewed by Schlosser, 2006), the PLLP migrates caudally along the body towards the tip of the tail. During the course of this migration, it deposits small clusters of cells, the proneuromasts, at its trailing edge. Each of these proneuromasts proceeds to differentiate into a functional neuromast. How is the stereotypical deposition of these neuromasts achieved? Three main mechanisms are involved in this process – the regulation of PLLP migratory behaviour, the specification of cells to become part of the proneuromast clusters, and the precise separation of migratory and non-migratory tissues.

The overall caudal migration of the PLLP is dependent on chemokine signalling. Migrating cells of the PLLP express the chemokine receptor CXCR4, whereas its ligand stromal-derived factor 1 (SDF1) is present in a narrow stripe of cells stretching the entire length of the body along which the PLLP migrates. Morpholino-induced knock-down of either CXCR4 or SDF1 results in the inhibition of PLLP migration (David et al., 2002). In addition, migratory characteristics of individual cells within the PLLP are regulated by the level of CXCR4 expression, which is highly expressed in migrating cells, less highly in trailing cells and only weakly in recently deposited cells, with expression lacking completely in proneuromasts (Gompel et al., 2001). Recent work has also demonstrated the presence of other chemokine receptors in the PLLP (Dambly-Chaudière et al., 2007; Valentin et al., 2007) as well as the heterogeneous expression of CXCR4 (Haas and Gilmour, 2006), but a consensus concerning the mechanisms of action involved remains to be established.

Prospective hair cells within proneuromasts appear to be determined by the progressive restriction of proneural and neurogenic gene expression. In particular, the proneural genes *atoh1* (the zebrafish *atonal* homologue) and *neuroD*, as well as the neurogenic genes *deltaA*, *deltaB* and *notch3* become selectively

expressed in cells that later acquire hair cell identity (Itoh and Chitnis, 2001; Sarrazin et al., 2006). Furthermore, the expression of *eyes absent 1* (*eya1*) has been shown to be necessary for the survival of prospective hair cells (Kozlowski et al., 2005). During migration of the PLLP, proneuromast cells arrange into cellular rosettes, each associated with Delta expression (Itoh and Chitnis, 2001) (reviewed by Ghysen and Dambly-Chaudière, 2007). These cellular rosettes periodically partition from the trailing end and are deposited along the migratory path.

Two recent reports have shown that the organization of the zebrafish PLLP is regulated by a fibroblast growth factor (FGF)-dependent signalling process that controls rosette formation, *atoh1* expression and migration of the primordium (Nechiporuk and Raible, 2008; Lecaudey et al., 2008). As shown in these studies, rosette formation occurs normally, and neuromast number is not reduced upon knock-down of *atoh1* or upon interference with Notch/Delta signalling. This finding lends support to the idea that FGF3/10 signalling acts as the common organizing principle in PLLP tissue morphogenesis that functions upstream of hair cell specification and of rosette formation.

The formation of cellular rosettes is involved in tissue morphogenesis during *Drosophila* germ band elongation (Blankenship et al., 2006). The generation of multicelluar rosettes and their subsequent resolution causes germ band cells to rearrange from a bilateral into a more anterior-posterior distribution. Rosette formation and resolution also involves the dynamic remodelling of asymmetrically distributed adherens junctions proteins and F-actin along dorsoventral and anterior-posterior cell–cell interfaces. Formation of multicellular rosettes has also extensively been studied in *Drosophila* compound eye development. Within the region of the morphogenetic furrow that progresses across the eye field, subsets of cells constrict their apical membranes, undergo shape changes and epithelial reorganization, which results in the formation of rosettes that pre-figure the differentiated ommatidia (reviewed by Wolff and Ready, 1993). The molecular and cell biological mechanisms underlying the cell shape changes and epithelial reorganization within the morphogenetic furrow are largely unknown. Recently, the regulation of cellular adhesion molecules via the proneural transcription factor Atonal and Epidermal growth factor receptor (EGFR) signalling has been shown to be involved in rosette formation (Brown et al., 2006).

In this study, we have investigated the subcellular dynamics underlying cellular rosette formation within the zebrafish PLLP. We show that this process involves the dynamic remodelling of apical membranes and the enrichment of apical junction proteins into focal points, a process that, in part, is regulated by the cell polarity regulators Lethal giant larvae 2 (Lgl2) and its ortholog Lgl1 (Sonawane et al., 2005). Our results provide further evidence that epithelial organization of the PLLP is required for the maturation of apical membranes, which in turn is essential for organizing cells into tightly adjoined rosettes that separate from surrounding tissues via differentially adhesive forces.

Results

Apical membrane constriction and cell shape changes during proneuromast rosette formation

During migration, the PLLP comprises ~100 cells that are organized as a compact migratory tissue (Ghysen and Dambly-Chaudière, 2004; Haas and Gilmour, 2006; Ghysen and Dambly-Chaudière, 2007). To visualize the subcellular dynamics of rosette formation within the PLLP, we performed immunohistochemical stainings at 32-36 hpf using antibodies against the apical markers atypical protein kinase C (PRKC; previously known as aPKC) (Horne-Badovinac et al., 2001; Peterson et al., 2001), zonula occludens 1 (ZO1), as well as actin. The PRKC antibody recognizes both the PRKCiota (PRKCi) and PRKCzeta (PRKCz) isoforms. In addition, we used a mouse monoclonal antibody that recognizes the cytoplasmic domain of human E-cadherin, which is highly conserved among other cadherins and therefore may not be E-cadherin specific. At the leading (distal) edge of the PLLP, ZO1 was not detected (Fig. 1A; Fig. 1A′, inset), whereas E-cadherin and PRKC were distributed among all intercellular membranes (Fig. 1A,C). Actin was also localized to intercellular membranes, but, in contrast to E-cadherin and to PRKC, it appeared highly enriched within spotted apical bands along anterior-posterior interfaces (Fig. 1B, white arrowheads). γ-Tubulin-positive centrosomes were arranged close to apical junctions belts within the plane of the epithelium (Fig. 1D). Towards the trailing (proximal) edge, the PLLP displayed two or three cellular rosettes. Within these rosettes, cells exhibited apical ZO1- (Fig. 1A; Fig. 1A′, inset), PRKC- and actin-rich focal points, and had acquired bottlenecked shapes (Fig. 1A-C). Throughout the entire PLLP, E-cadherin was uniformly localized among all intercellular membranes and was not enriched within apical focal points. Three-dimensional reconstructions of confocal *z*-stack images revealed that apical focal points were associated with presumptive hair cells that were positioned below the plane of the epithelial layer. These presumptive hair cells were recognized by the deep nuclear label (see white asterisks within red and green insets in Fig. 1A,B) and by Delta D expression (see below). Consistent with a strong polarization of rosette cells, centrosomes were localized close to the apical side, whereas nuclei were localized to the opposite basal sides of rosette cells (Fig. 1D). Individual rosettes were surrounded by presumptive inter-neuromast cells. These results indicate that PLLP cells undergo strong apicobasal polarization, size restriction of apical membranes and cell shape changes during rosette formation. In addition, rosette formation appears to proceed from the leading (distal) towards the trailing (proximal) edge of the PLLP.

Apical membrane maturation corresponds with Delta/Notch-mediated hair cell progenitor specification

Delta/Notch signalling between hair cell progenitors and surrounding support cells pre-patterns the PLLP prior to neuromast deposition (Itoh and Chitnis, 2001). To further characterize the correlation between apical membrane maturation and the Delta/Notch pattern that underlies hair cell progenitor and support cell formation within presumptive neuromasts (Itoh and Chitnis, 2001; Ghysen and Dambly-Chaudiere, 2004), we characterized hair cell progenitor distribution using an antibody against Delta D and assessed rosette formation using antibodies against PRKC or β-catenin (Itoh et al., 2003). As a result, Delta D immunoreactivity was confined to one or two presumptive hair cells within each rosette. Moreover, we found that Delta D-positive aggregates associated with, but did not colocalize with, apical focal points (Fig. 2A,B). Three-dimensional reconstructions of confocal *z*-stacks revealed that the nuclei of Delta D-positive presumptive hair cells were positioned beneath each apical focal point. Our findings are consistent with two recent reports that also described a strong correlation between rosette formation and Delta/Notch patterning (Nechiporuk and Raible, 2008; Lecaudey et al., 2008). However, as shown by these two studies, Delta/Notch signalling is apparently not required for rosette formation, which can occur in the absence

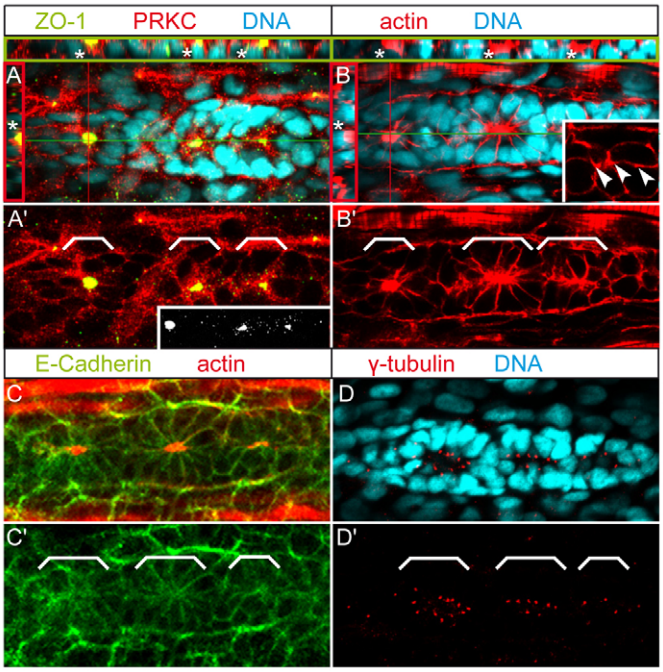

Fig. 1. Epithelial organization and apical membrane constriction during PLLP rosette formation. Epithelial organization of PLLP cells was assayed by immunohistochemistry. Shown are reconstructions of confocal images of the PLLP at 36 hpf. (A,B) Asterisks indicate nuclei of deep cells underlying apical focal points. Red lines indicate cross-section planes, green lines indicate sagittal section planes, and the respective sections are shown within red (apical towards the left) or green insets (apical towards the top). White brackets indicate positions of individual rosettes. Cross- and sagittal sections reveal that ZO1- and actin-rich constrictions are apical, and that single presumptive hair cells are below the plane of the epithelial layer (recognized by the deep nuclear staining). Inset in A′ depicts ZO1, which localizes to apical focal points but is not detectable along other cell membranes, including the leading edge region. (B) White inset shows details of the leading edge region, which contains apical actin spots along anterior-posterior interfaces (white arrowheads). Dynamic apical constriction of actin and apical ZO1 localization occur in a leading to trailing edge direction. (C,C′) E-Cadherin does not cluster within apical constrictions. (D) Centrosomes are arranged closely around apical constrictions. White brackets indicate positions of individual rosettes.

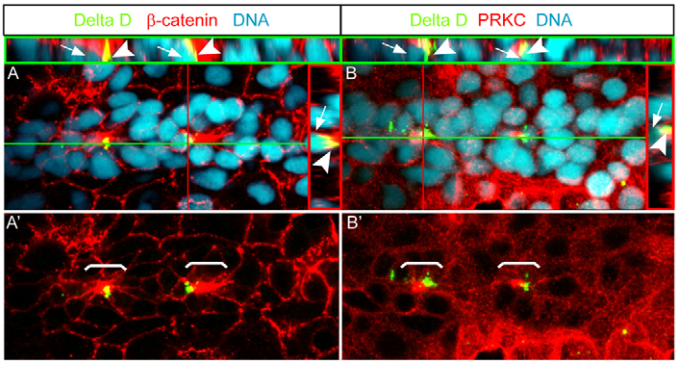

Fig. 2. Apical membrane constriction corresponds with Delta/Notch-mediated hair cell progenitor specification. Epithelial organization of PLLP cells, as assayed by immunohistochemistry. Shown are reconstructions of confocal images of the PLLP at 36 hpf. Red lines indicate cross-section planes, green lines indicate sagittal section planes and the respective sections are shown within red (apical to the right) or green insets (apical to the top). White brackets in A′ and B′ indicate position of individual rosettes. Individual rosettes contain apical (A) β-catenin- and (B) PRKC-rich apical focal points that are associated with Delta D. White arrowheads (red and green insets) indicate Delta D-positive aggregates that are associated with apical constrictions but extend more basolaterally towards the nuclei of the deep hair progenitor cells (white arrows).

of hair cell progenitors. These functional studies and our results suggest that rosette formation and hair cell progenitor specification are independent, but tightly coupled, processes.

Dynamics of neuromast deposition

To assess whether cellular rosettes are indeed proneuromasts that are periodically deposited from the PLLP during migration, we labelled wild-type embryos with the membrane marker BODIPY ceramide (Cooper et al., 1999) and performed time-lapse analysis over a 3-hour period. Individual rosettes were identified by the presence of apical membrane condensations and bottlenecked cell shapes, and by their overall tissue organization. During tissue separation, the migratory speed of the trailing cellular rosette, including the surrounding presumptive interneuromast cells, declined and the rosette complex lagged behind the PLLP. During tissue separation, rosette cells and their surrounding presumptive interneuromast cells displayed elongated shapes, in accordance with predicted pulling forces expected to act upon these cells during tissue separation (Fig. 3). Importantly, tissue separation never occurred within rosettes. Instead, rosettes were separated exclusively in between presumptive interneuromast cells (n=8 embryos analyzed). These observations demonstrate that cellular rosettes are indeed proneuromasts and function as units of tissue separation.

Maturation of apical focal points is redundantly controlled by Lgl1 and Lgl2

Time-lapse and immunohistochemical analysis both suggested that apical focal points ensure increased affinity among rosette cells compared with cell-cell contacts between inter-neuromast cells. To functionally characterize the maturation of apical focal points, we analyzed mutants that affect cell polarity and apical junction formation. The zebrafish mutations *heart and soul* (*has*)/*prkci* and *penner*, which encodes the zebrafish homolog of Lgl2, affect cell polarity and epithelial maintenance (Horne-Badovinac et al., 2001; Peterson et al., 2001; Horne-Badovinac et al., 2003; Sonawane et al., 2005; Rohr et al., 2006). At 28-32 hpf, both *lgl2* and *has*/*prkci* were expressed within the PLLP, which suggested a role in PLLP epithelial organization (Fig. 4A,B). Zygotic *penner*/*lgl2* mutants lack obvious defects prior to 72 hpf, presumably owing to a strong maternal contribution (Sonawane et al., 2005). We therefore produced three antisense morpholino oligonucleotides ($MO^{lgl2\text{-}atg}$; $MO^{lgl2\text{-}utra}$; $MO^{lgl2\text{-}utrb}$) designed to interfere with maternal mRNA translation (Nasevicius and Ekker, 2000). To investigate the role of PRKCI in neuromast formation, we characterized embryos injected with MO^{prkci}. To avoid the major off-targeting effects of MOs that are mediated through p53 activation, we also co-injected MO^{p53} (Langheinrich et al., 2002; Robu et al., 2007). Efficacy of the *lgl2* knockdown was tested by co-injecting a reporter construct that expresses mRNA encoding eGFP-tagged Lgl2 and $MO^{lgl2\text{-}atg}$. Embryos injected with the reporter construct alone strongly expressed the membrane-associated fusion protein (n=27/35), whereas Lgl2::eGFP expression was absent in all embryos co-injected with $MO^{lgl2\text{-}atg}$ (n=0/32) (Fig. 4C,D). Although the efficacy of the other *lgl2* MOs could not be tested with the *lgl2::eGFP* reporter construct, owing to the lack of sequence complementarity,

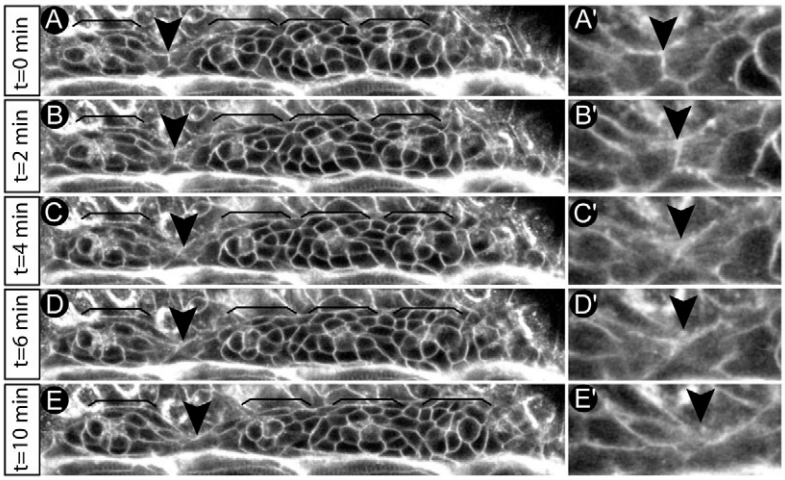

Fig. 3. Dynamics of neuromast deposition. (A-E′) Shown is the process of neuromast deposition within a wild-type embryo that was labelled with the vital membrane marker BODIPY ceramide and followed over a 10-minute period by time-lapse analysis. Rosettes are indicated by brackets and the plane of tissue separation is indicated by arrowheads. (A′-E′) Details of cellular cell shape changes along the plane of tissue separation indicate that cells surrounding individual rosettes are extensively elongated and that tissue separation occurs exclusively in between interneuromast cells, leaving individual rosettes intact. Therefore, rosettes, including their surrounding cells, are units of tissue separation.

the three MOs produced identical morphant phenotypes. Injection of MO^{prkci} produced a phenotype that matched the morphological aspects of *has*/*prkci* mutants.

To assess systematically whether maturation of apical focal points within the PLLP depends on Lgl or PRKC, we co-injected embryos either with MO^{p53}/MO$^{lgl2\text{-}utrb}$ or MO^{p53}/MO^{prkci}. We preferred MO$^{lgl2\text{-}utrb}$ for combination with other MOs, as it exerted a robust morphant phenotype at a concentration of 70 μmol/l in comparison with the other two *lgl2* MOs (which required injections at concentrations of 100 μmol/l). To test whether functional redundancies exist between *lgl2* and its ortholog gene *lgl1*, between *prkci* and *prkcz* (Cui et al., 2007), or between *lgl2* and *prkci*, we also injected the corresponding triple MO combinations MO^{p53}/MO$^{lgl2\text{-}utrb}$/MO^{lgl1}, MO^{p53}/MO$^{lgl2\text{-}utrb}$/MO^{prkci}, or MO^{p53}/MO^{prkci}/MO^{prkcz}. The efficiency and specificity of the MO^{lgl1} was verified by western blot using an antibody against the C terminus of *Xenopus* Lgl1 (Dollar et al., 2005) and by mRNA rescue experiments (supplementary material Fig. S1). We also included a MO^{p53} only-injected control group to reassure ourselves about the specificity of the observed effects. To quantify the effects on cellular morphogenesis and on rosette formation, morphants were double-labelled with an antibody against ZO1 and rhodamine phalloidin, which labels filamentous actin (Fig. 5A; data not shown). Whereas in wild-type and MO^{p53} morphants, apical ZO1-positive junction belts increased considerably in size during the progression of cellular rosettes from leading towards trailing edge positions, maturation of apical focal points was severely affected in MO^{p53}/MO^{lgl1}/MO$^{lgl2\text{-}utrb}$ triple morphants (Fig. 5A,B). Comparative quantification of ZO1-positive areas was carried out on confocal image *z*-stack projections employing the ImageJ particle analysis function. This analysis revealed that the average total area of all focal points/PLLP and the average area of the apical focal points closest to the trailing edge was significantly diminished in MO^{p53}/MO^{lgl1}/MO$^{lgl2\text{-}utrb}$ triple morphants compared with wild-type and MO^{p53} morphants (Fig. 5B,C). By comparison, no statistically significant compound effects were observed for any other combination of MOs analyzed, although MO^{p53}/MO$^{lgl2\text{-}utrb}$ double morphants and MO^{p53}/MO^{prkci}/MO$^{lgl2\text{-}utrb}$ triple morphants displayed a tendency to have smaller apical focal point areas (Fig. 5B,C). These findings suggest a functional redundancy between *lgl1* and *lgl2* in controlling the maturation of apical focal points.

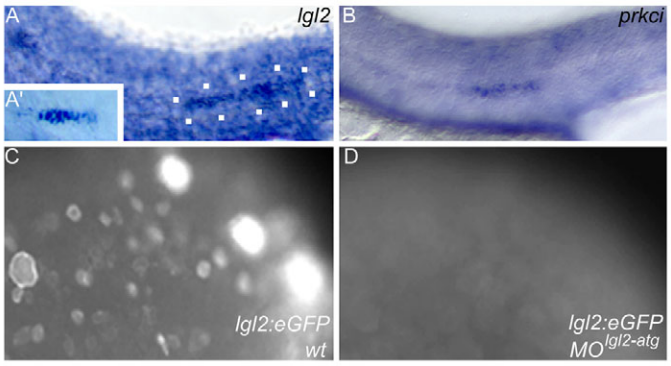

Fig. 4. *lgl2* and *prkci* expression within the posterior lateral line. (A,B) Expression of *lgl2* and *prkci* within the PLLP at 28-32 hpf (PLLP outlined with white dots) and (A′) *lgl2* expression within the secondary primordium of the lateral line organ at 48 hpf. (C) Injection of a reporter plasmid expressing Lgl2::eGFP results in strong protein expression during gastrula stages in wild type but (D) is efficiently blocked in MO$^{lgl2\text{-}atg}$ injected animals.

Maturation of apical focal points affects the number of rosettes within the PLLP and the pattern of neuromast deposition

Defective maturation of apical focal points in embryos lacking Lgl1 and Lgl2 may affect the formation of cellular rosettes within the PLLP. We therefore assessed whether the formation of cellular rosettes within the PLLP was affected in embryos lacking both Lgl1 and Lgl2, and compared the effects observed with those present in other morphants or in wild type. Quantifications of cellular rosettes that were detected based on actin and apical ZO1-positive focal points within the trailing region of the PLLP revealed that, on average, wild-type and MO^{p53} morphants contained a number of rosettes at 30 hpf, which was comparable with the number of rosettes present in MO$^{lgl2\text{-}utrb}$/MO^{p53}, MO^{lgl1}/MO^{p53}, MO^{prkci}/MO^{p53} or MO^{prkcz}/MO^{p53} double morphant embryos (Fig. 5D). Consistent with a redundant function of Lgl1 and Lgl2 in controlling the maturation of apical focal points, MO^{p53}/MO^{lgl1}/MO$^{lgl2\text{-}utrb}$ triple morphants had significantly fewer cellular rosettes within the trailing region of PLLPs (Fig. 5D). This finding suggests that Lgl-mediated maturation of apical membranes affects rosette formation. By contrast, loss of both, PRKCi and PRKCz, did not cause a significant reduction in the number of cellular rosettes within the PLLP.

Although knock-down of *lgl2* alone did not produce significant changes in the number and maturation of cellular rosettes within

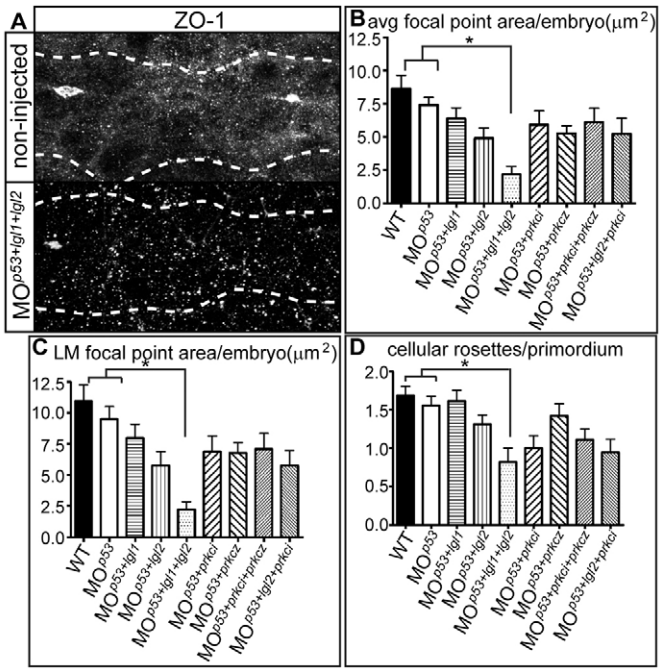

Fig. 5. Apical focal point area is affected by Lgl2 and Lgl1. (A) Apical focal points and the migrating PLLP (outlined by white dots) were visualized by immunohistochemistry using an antibody against ZO1 as well as rhodamine-phalloidin (not shown) in wild-type and MO^{p53}/MO$^{lgl2\text{-}utrb}$/MO^{lgl1}-injected 34 hpf embryos. MO^{p53} was co-injected to minimize off-target effects. (B,C) The size of ZO1-positive areas was analyzed quantitatively. Both the averaged total focal point area and the area of the left-most (LM) proximal focal point are significantly reduced (considered to be significant if P<0.05) in MO^{p53}/MO$^{lgl2\text{-}utrb}$/MO^{lgl1}-injected morphants when compared with wild-type or MO^{p53}-injected morphants (P<0.001 compared with wild type and P<0.01 compared with MO^{p53}). (D) The average number of cellular rosettes/PLLP. The number of rosettes is strongly reduced in MO^{p53}/MO$^{lgl2\text{-}utrb}$/MO^{lgl1} morphant embryos compared with wild-type or MO^{p53} morphants. The following number of embryos was analyzed: wild type, n=16; MO^{p53}, n=18; MO^{p53}/MO^{lgl1}, n=13; MO^{p53}/MO$^{lgl2\text{-}utrb}$, n=16; MO^{p53}/MO$^{lgl2\text{-}utrb}$/MO^{lgl1}, n=11; MO^{p53}/MO^{prkci}, n=20; MO^{p53}/MO^{prkcz}, n=19; MO^{p53}/MO^{prkci}/MO^{prkcz}, n=18; MO^{p53}/MO$^{lgl2\text{-}utrb}$/MO^{prkci}, n=18. Error bars indicate s.e.m.

PLLPs, we speculated that subtly defective maturation of apical focal points may decrease the affinity between rosette cells or among interneuromast cells, and thereby affect the precise deposition of neuromasts from the trailing edge. To assess this potential link between apical focal point maturation and neuromast deposition, we analyzed the spatial distribution of neuromasts in wild type, MO^{p53} morphant and MO$^{lgl2\text{-}utrb}$/MO^{p53} double morphant embryos at 48 hpf. At this stage, all neuromasts have been deposited by the PLLP and were recognized using the membrane marker BODIPY ceramide or the *eyes absent 1* (*eya1*) in situ hybridization probe (Sahly et al., 1999). To quantify the effects on neuromast distribution, first the average position for each of the first four neuromasts was determined and then the standard deviation for each position was taken as an indication of the distribution range. According to this analysis, loss of Lgl2 generally resulted in more posterior average neuromast positions compared with wild type. In addition, embryos injected with MO^{lgl2}/MO^{p53} displayed a significantly wider spread in the distribution of neuromasts within the posterior lateral line organ compared with wild type or MO^{p53} morphants (Fig. 6). Therefore, loss of Lgl2 disturbs the precise distribution of neuromasts along the tail during morphogenesis of the posterior lateral line organ. This finding suggests that tissue organization and rosette formation affect the correct morphogenesis of the posterior lateral line organ.

Evidence for PRKCi signalling via Lgl2 during PLLP apical membrane maturation

In a variety of cellular contexts, PRKCi regulates Lgl2 function by phosphorylation events within the central Lgl domain of the protein which render Lgl2 inactive (Betschinger et al., 2003; Plant et al., 2003; Yamanaka et al., 2003; Betschinger et al., 2005). According to this model, non-phosphorylatable Lgl2^{S5A} protein (Ser643, Ser647, Ser651, Ser658 and Ser661 within the Lgl domain exchanged for Ala residues) should be constitutively active. To confirm this, we injected embryos with 100 pg of synthetic mRNA that encodes Lgl2^{S5A} protein. Owing to low levels and mosaic expression of the mutant protein, we recovered only a fraction of embryos with defective PLLPs. Similarly, upon mRNA injection, we recovered only a small fraction of embryos expressing a dominant inhibitor of PRKCi (kinase dead PRKCi^{KD}, residues Pro408 and Glu409 within the catalytic centre exchanged for Ala residues) (Rohr et al., 2006). However, both mutant embryos displayed PLLP phenotypes that were even stronger than those of MO^{p53}/MO^{lgl1}/MO$^{lgl2\text{-}utrb}$ triple morphants and resulted in fewer cellular rosettes with actin, ZO-1 and PRKCi-rich apical focal points (Fig. 7C-F). Lack of rosette formation coincided with a failure of cells to acquire bottlenecked shapes, to translocate nuclei to one side and to arrange centrosomes close to the opposite side. Actin, PRKC and E-cadherin were localized along all cell membranes, whereas ZO1 was not detectable. Therefore, altered activity of Lgl2 or PRKCi using constitutively active or dominant-negative forms of these proteins, respectively, results in a severe delay or complete failure of PLLP cells to constrict apical membranes, to acquire bottlenecked shapes and to arrange into cellular rosettes (Fig. 7G; supplementary material Fig. S2). The phenotypic similarities between embryos injected with either one of the mutant mRNAs suggest that regulation of Lgl activity by altering PRKCi signalling affects the formation of apical focal points. The severity of the Lgl2^{S5A} mutant phenotype, which is comparable or even stronger than the MO^{p53}/MO^{lgl1}/MO$^{lgl2\text{-}utrb}$ triple morphant phenotype, indicates that the overexpression of a mutant form of Lgl2 may also interfere with maternal protein and with its ortholog Lgl1 (Sonawane et al., 2005). Our findings imply that rosette formation and epithelial morphogenesis within the PLLP requires apicobasal cell polarity cues.

Discussion

Here, we have described the tissue dynamics that underlie organization and precise deposition of proneuromasts within the zebrafish PLLP. Our results demonstrate that the PLLP is a migratory epithelial tissue, as evidenced by the polarized distribution of epithelial junctional proteins and by the tight association of PLLP cells via junctional adhesion belts. This finding supports previous analyses that have implied such a tissue organization based on gene expression and on the epidermal placodal origin of the primordium (Kollmar et al., 2001; Liu et al., 2003; Lopez-Schier et al., 2004; Kerstetter et al., 2004; Haas and Gilmour, 2006; Wilson et al., 2007). Consistent with two other reports, we have found now that cells within the PLLP exhibit dynamic remodelling of apical cell-cell contacts during the generation of proneuromast cell rosettes (Nechiporuk and Raible, 2008; Lecaudey et al., 2008). Our data extends these two studies by showing that the epithelial cell

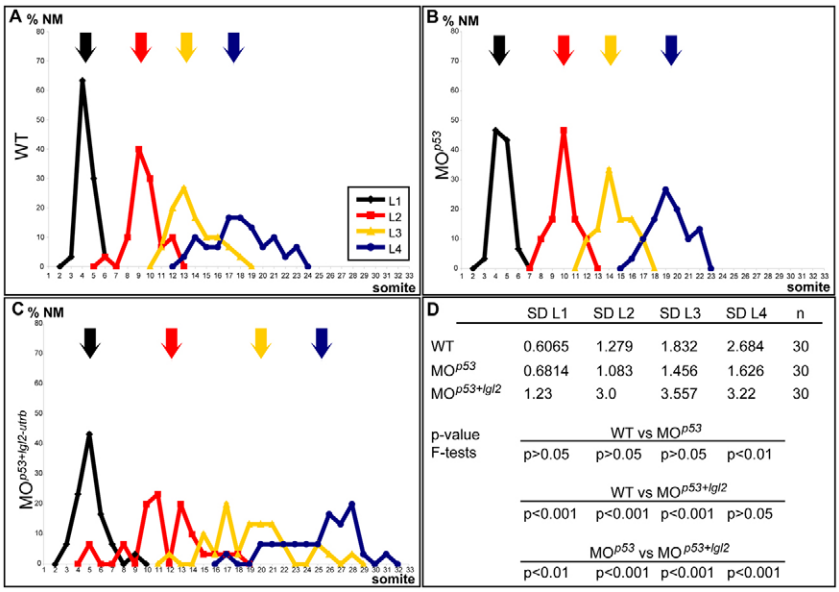

D

	SD L1	SD L2	SD L3	SD L4	n
WT	0.6065	1.279	1.832	2.684	30
MO^{p53}	0.6814	1.083	1.456	1.626	30
$MO^{p53+lgl2}$	1.23	3.0	3.557	3.22	30

p-value F-tests				
WT vs MO^{p53}	p>0.05	p>0.05	p>0.05	p<0.01
WT vs $MO^{p53+lgl2}$	p<0.001	p<0.001	p<0.001	p>0.05
MO^{p53} vs $MO^{p53+lgl2}$	p<0.01	p<0.001	p<0.001	p<0.001

Fig. 6. Distribution of the first four neuromast positions is affected by loss of Lgl2. Schematic representation of the distribution of the first four neuromast positions, L1-L4, in (A) wild-type, (B) MO^{p53}- and (C) MO^{p53}/$MO^{lgl2\text{-}utrb}$-injected embryos at 48 hpf. The arrows indicate the mean positions of L1-L4 based on the following calculated means: (A) wild type (n=30): L1, 4.333; L2, 9.533; L3, 13.766; L4, 17,966; (B) MO^{p53} (n=30): L1, 4.533; L2, 10.000; L3, 14.466; L4, 19.333; (C) MO^{p53}/$MO^{lgl2\text{-}utrb}$ (n=30): L1, 5.066; L2, 11.633; L3, 19.366; L4, 25.1. (D) The standard deviation (s.d.) of each population from these means is provided, as well as the P values of the F-test performed to determine whether any difference in the s.d. is statistically significant (considered to be the case if P<0.05). The spread of the distribution of the mean position is significantly wider for each of the first four neuromasts in MO^{p53}/$MO^{lgl2\text{-}utrb}$-injected embryos when compared with MO^{p53}-injected embryos.

polarity regulator Lgl2, together with its ortholog Lgl1, is a potential downstream effector of FGF signalling that mediates the strong polarization of cells along their apicobasal axes and controls the size restriction of apical membranes, the growth of apical ZO1-, actin- and PRKC-rich focal accumulations, the apical localization of centrosomes, and the basal localization of nuclei. The tight constriction of apical membranes and enrichment of apical proteins into apical focal points is suggestive of a function of these structures as nucleation points for cell rosettes and as adhesive links during tissue separation. Such nucleation points could generate selective adhesion forces that are stronger among cells within proneuromast rosettes than among interspersed interneuromast cells. In our study,

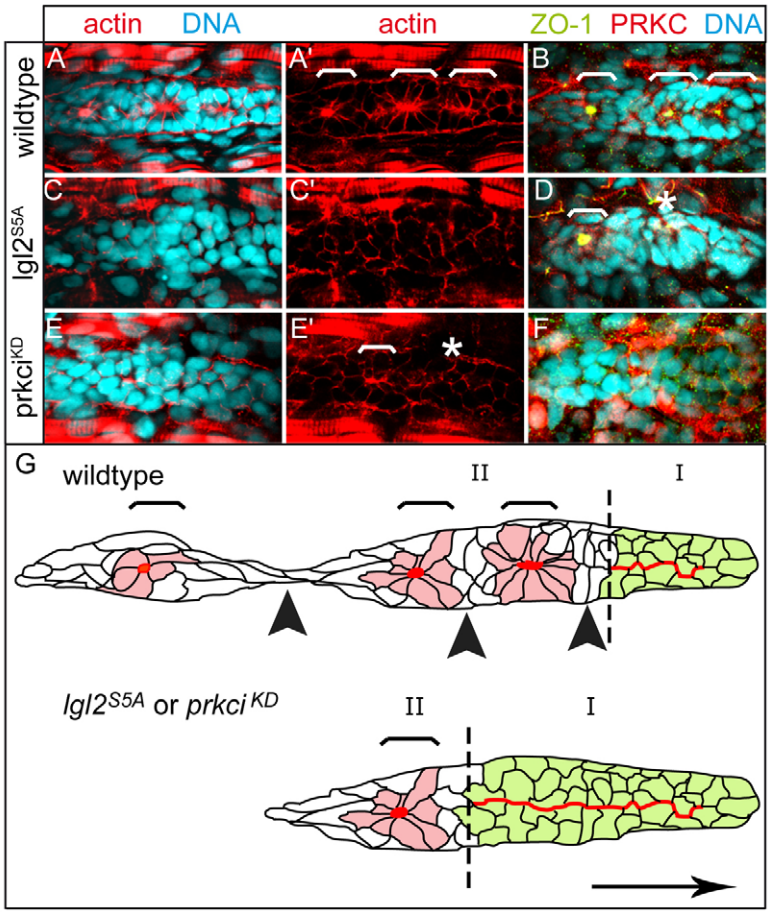

Fig. 7. Apical membrane constriction and rosette formation is affected by antagonistic activities of Lgl2 and PRKCi. Epithelial organization of PLLP cells was assayed by immunohistochemistry. Shown are reconstructions of confocal images of the PLLP at 36 hpf. (A-F) The number of rosettes (white brackets) is strongly reduced within different backgrounds. (E′) Instead, the central region of the PLLP frequently contains actin-rich spots that are indicative of incomplete apical constriction (white asterisks). (F) Loss of ZO1 expression within severely affected PLLPs that fail to produce rosettes. There is mosaic and strong ectopic expression of $PRKCi^{KD}$ upon overexpression of the corresponding mRNA. (G) Schematic diagram of tissue separation within the PLLP. Red indicates the distribution of actin-rich apical membranes that are widely present within the leading edge region of the PLLP (green cells, region I) and confined to apical focal points within rosettes (light red cells, region II; regions indicated by broken line), which are surrounded by interneuromast cells (white cells). In $lgl2^{S5A}$ or $prkci^{KD}$ mutants, the process of rosette formation is delayed. Brackets indicate presumptive neuromasts and black arrowheads indicate future points of tissue separation. The direction of PLLP migration is indicated by a black arrow.

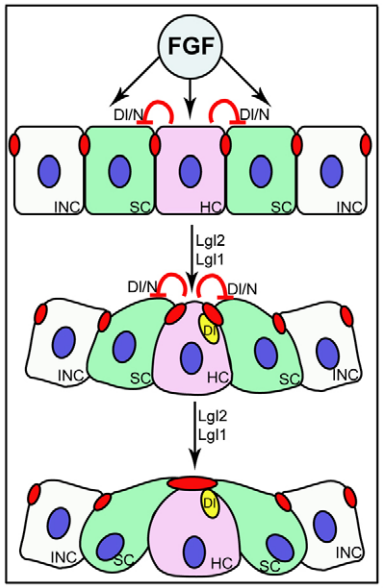

Fig. 8. Possible scenario illustrating the process of rosette formation. FGF signalling most probably links tissue morphogenesis regulated by Lgl2 and Lgl1 with the Dl/N interaction involved in hair cell specification. Delta/Notch activity (Dl/N) singles out a Delta D-positive hair cell progenitor (HC, pink) among a group of presumptive support cells (SC, green). Delta D-positive aggregates (yellow ovals) associate with but do not colocalize with actin-rich adhesion complexes (red ovals). Each rosette is surrounded by a group of interneuromast cells (INC, white) that do not undergo apical clustering. Activity of the cell polarity regulators Lgl2 and Lgl1 is required for maturation of apical junctions.

we could indirectly substantiate this hypothesis by live imaging of the PLLP, which revealed that, during neuromast deposition, tissue separation occurs exclusively among interneuromast cells and that substantial pulling forces are involved in this process (as evidenced by their elongated cell shapes). Previous studies have shown that loss of cadherin 2 (N-cadherin) affects neuromast formation (Kerstetter et al., 2004; Wilson et al., 2007). This finding provides additional evidence in support of our study, which shows that the epithelial organization of the PLLP is essential for correct tissue morphogenesis.

Delta/Notch signalling has been implicated in pre-patterning the PLLP prior to neuromast deposition (Itoh and Chitnis, 2001; Sarrazin et al., 2006). Here, we have shown that Delta D-positive aggregates mark presumptive hair cells and using this marker, we could demonstrate that the formation of proneuromasts involves the arrangement of one or two Delta D-positive hair cell progenitor(s) and several surrounding support cells into cellular rosettes. Interestingly, interneuromast cells that are interspersed in between proneuromast cells and are not in direct contact with hair cell progenitors, do not exhibit obvious cell shape changes, rosette formation or remodelling along their apicobasal axis.

Previous studies have shown that the PLLP is pre-patterned into leading versus trailing end cell populations that are defined by expression of distinct chemokine receptors or of the Met receptor tyrosine kinase, and that this organization is crucial for precise tissue separation (Haines et al., 2004; Dambly-Chaudière et al., 2007; Valentin et al., 2007). Our study complements these analyses and provides insight into the cellular behaviours and tissue dynamics underlying this complex morphogenetic process. We could show that the formation of apical focal points and epithelial morphogenesis, in part, is controlled by the cell polarity regulators Lgl2 and Lgl1. We find that defective apical membrane maturation corresponds with an aberrant proneuromast deposition pattern. We currently have no explanation except that the precise timing of tissue separation may be controlled by adhesive forces that are in place between interneuromast cells, which may be affected in *lgl2* morphants. The role of the Lgl2 antagonist PRKCi remains to be further characterized. Defective PRKCi signalling via Lgl2, as assessed using the overexpression of dominant-negative kinase-dead and phosphorylation-deficient mutant forms of both proteins, respectively, completely abrogates the formation of rosettes within the PLLP and, correspondingly, prevents proneuromast deposition. It remains to be shown whether this effect is due to interference with maternal pools of PRKCs or whether the PRKCi dominant-negative effects are due to misregulation of Lgl2 function. Together, our results indicate the importance of cellular polarity in PLLP tissue organization.

Similar to our conclusions, epithelial rosette formation during *Drosophila* germ band elongation has been implicated in tissue reorganization during morphogenesis (Blankenship et al., 2006). However, in contrast to the processes described here, rosettes that appear during *Drosophila* germ band elongation are transient structures that are associated with the rearrangement and movement of epithelial cells during gastrulation. Whereas proneuromast rosettes are permanent groups of cells that are not separable, Blankenship and colleagues have shown that a single cell can contribute to different rosettes over time. These differences in the rosettes are further substantiated by the finding that proneuromast rosette formation involves the apical constriction of membranes and that their formation is affected by mutations of genes that are known to regulate apico-basal cell polarity. By comparison, rosette formation within the *Drosophila* germ band is not restricted to the apical surfaces and appears to be more of a planar polarity phenomenon. Rosette formation within the zebrafish PLLP is apparently more similar to processes that occur within the morphogenetic furrow of the *Drosophila* eye field (Brown et al., 2006). However, in contrast to this system, in which proneural gene patterning directly or indirectly affects levels of adherens junctions components with the *Drosophila* compound eye, cellular rosette formation and epithelial remodelling within the zebrafish PLLP are independent of *atoh1* or Notch/Delta signalling (Nechiporuk and Raible, 2008; Lecaudey et al., 2008). Together, our studies and those of others (Nechiporuk and Raible, 2008; Lecaudey et al., 2008) suggest that rosette morphogenesis and specification of the central Delta-expressing cell surrounded by Notch-expressing cells are independent processes, and that FGF3/10 signalling links these two self-organizing events (Fig. 8). In the future, it will be interesting to elucidate further the molecular mechanisms by which FGF signalling activates the cell polarity machinery, which, in turn, directs tissue morphogenesis.

Materials and Methods

Fish maintenance and stocks

Zebrafish were maintained at standard conditions (Westerfield, 1994). Embryos were staged by hpf at 28.5°C (Kimmel et al., 1995) and according to somite number. The morphological and immunohistological analysis of *lgl2* morphants was carried out in the AB background.

DNA constructs and site-directed mutagenesis

The coding region of zebrafish *lgl2* was PCR amplified and cloned into the *Cla*I and *Xho*I restriction sites of the expression vector pCS2+. Similarly, the full-length coding region of *lgl1* was PCR amplified from cDNA and subcloned into pCS2+. The N-terminal myc-tag was generated by subcloning the constructs into pCS2+myc. Further

details are available upon request. IMAGp998C239110Q3 containing full-length *lgl2* was purchased from RZPD. Site-directed mutagenesis was performed using the Quick Change Site Directed Mutagenesis Kit (Stratagene, CA, USA). The pCS2+14xUAS *E1b lgl2:eGFP* (Koester and Fraser, 2001) was cloned by introducing the *Cla*I (blunt end)/*Xho*I fragment of *lgl2* into pCS2+ 14xUAS expression vector. The following mutagenesis primer sequences were used for *lgl2*^{S5A}: 5′-CACGAGTCAAG-**GCC**ATCAAAAAG**GCT**CTGCGACAG**GCC**TTCCGCAG-3′ and 5′-GATTCGC-CGC**GCT**CGAGTC**GCC**ATGCGCAAAC-3′. Bold nucleotides indicate changes from the wild-type sequence.

RNA and morpholino injections

DNA constructs were transcribed using the SP6 MessageMachine kit (Ambion). In vitro synthesized capped mRNA was dissolved in water and mixed with the MO prior to injection. Typically, 100 pg of RNA were injected into AB embryos for rescue and overexpression. MOs (Gene Tools) were injected at concentrations of 70 and 100 μmol/l.

MO sequences were: MO$^{lgl2\text{-}utra}$, 5′-TCCCTGGACGAGCCGGGACTCAAAC-3′; MO$^{lgl2\text{-}utrb}$, 5′-AGCCGGGACTCAAACTGCCCTCTCT-3′; MO$^{lgl2\text{-}atg}$, 5′-GCCCA-TGACGCCTGAACCTCTTCAT-3′; MO$^{lgl1\text{-}atg}$, 5′-CCGTCTGAACCTAAACTT-CATCATC-3′; MO$^{lgl1\text{-}utr}$, 5′-TGAAGCCGAATCAGAGGTAAATCAC-3′; MO^{prkci}: 5′-TGTCCCGCAGCGTGGGCATTATGGA-3′; MO^{prkcz}, 5′-GATCCGTTACTGA-CAGGCATTATA-3′; and MO^{p53}, 5′-GCGCCATTGCTTTGCAAGAATTG-3′.

In situ hybridization

Whole-mount in situ hybridization was performed as previously described (Jowett and Lettice, 1994). Digoxigenin-UTP labelled riboprobes were synthesized according to manufacturer's instructions (Boehringer Mannheim). The probe for *lgl2* was amplified from cDNA and subcloned into TOPO vector. The primers that were used were: 5′-CGGCTCGAGCTTGCTCACCTTCAC-3′ and 5′-CCCATAACTGG-CCCTCGGCATCCC-3′.

The probe for *eya1* was a gift from C. Petit. The probe for *met* was amplified from cDNA and subcloned into the TOPO vector. The following primers were used: 5′-CACTATTCTGAAGCTGCTTCCATCC-3′ and 5′-CGTGATGGAGATAAGGCA-AACGGC-3′

For documentation, embryos were dehydrated, cleared in benzyl:benzoate and mounted in Permount (Fisher Scientific). Images were captured using a Zeiss Axioplan 2 microscope using 10× and 20× lenses, and Metamorph imaging software version 6.1 (Visitron). Images were processed with Adobe Photoshop software (Adobe Systems).

Quantification of ZO1-positive areas was carried out on regions of interest (ROIs) of confocal image *z*-stack projections employing the ImageJ (http://rsb.info.nih.gov/ij/index.html) particle analysis function (parameters available on request). Statistical analysis was performed using one-way ANOVA. A *P* value of less than 0.05 was considered to indicate significance. Neuromast distribution analysis was performed on 48 hpf embryos. Statistical analysis was performed using two-way ANOVA or the F-test as appropriate. A *P*-value of less than 0.05 was considered to indicate significance.

All statistical analysis was carried out using GraphPad Prism 4 statistical software (GraphPad Software, La Jolla, CA, USA).

Immunohistochemistry, western blotting and phalloidin staining

Immunohistochemistry and phalloidin staining was performed as previously described (Horne-Badovinac et al., 2001). The Delta D and β-catenin immunohistochemical staining was performed by fixing embryos in 10% TCA followed by several rinses and permeabilization with 0.2% Triton X-100 for 30 minutes followed by blocking for 2 hours. Prior to mounting, stained tissue was transferred through a series of graded glycerol of 25%, 50% and 75%. For western blotting, we used essentially same protocol as previously described (Horne-Badovinac et al., 2001) using embryonic tissues staged to 24-30 hpf.

The following antibodies were used: rabbit anti-aPKCζ (1:200, Santa Cruz Biotechnology, USA); mouse anti-ZO1 (1:200, Zymed); mouse anti-human E-cadherin (1:200, BD Biosciences Pharmingen, Material Number 610182); mouse anti-γ-tubulin (1:200, Biozol); mouse anti-Delta D (1:400) (Itoh et al., 2003); rabbit anti-β-catenin (1:600, a gift from the Birchmeier laboratory); rabbit anti-*Xenopus* Lgl1 C terminus (a gift from the Sokol laboratory) (Dollar et al., 2005); and goat anti-mouse RRX (1:200), anti-rabbit Cy5 (1:200), anti-mouse Cy5 (1:200) and anti-rabbit Cy2 (1:200) (Jackson ImmunoResearch). Nuclear staining was performed using 4′6-diamidino-2-phenylindole, dihydrochloride (1:1000, FluoroPure grade). Confocal images were obtained with the Zeiss LSM510 META confocal microscope using a Plan Neofluar 100× oil immersion lens and zoom 1.0. Confocal images and three-dimensional reconstructions of *z*-stacks were performed using the LSM 510 Meta software. Images were processed using Photoshop software (Adobe).

Time lapse imaging

Prior to live imaging, embryos were incubated with 100 μM of the vital dye BODIPY ceramide (Molecular Probes) in Danieau's for 1 hour. Embryos were mounted in 1.8% low melting agarose and anesthetized with Tricain (Sigma) and imaged using the Zeiss LSM510 META confocal microscope using a Plan Neofluar 40× oil immersion lens and zoom 1.0.

We thank C. Birchmeier-Kohler, C. Dahm and members of the Abdelilah-Seyfried laboratory for their critical comments on the manuscript. We are indebted to W. Birchmeier, R. Köster, C. Petit and S. Sokol for sharing reagents and tools. R. Fechner was an excellent help in the maintenance and technical assistance of our fish facility. We apologize to colleagues whose work may not have been mentioned in this study. This work was supported by a presidential grant of the Helmholtz society towards the Berlin Institute for Heart Research (BIHR) to D.H. and from the Volkswagen Stiftung to S.A.-S.

References

Betschinger, J., Mechtler, K. and Knoblich, J. A. (2003). The Par complex directs asymmetric cell division by phosphorylating the cytoskeletal protein Lgl. *Nature* **422**, 326-330.

Betschinger, J., Eisenhaber, F. and Knoblich, J. A. (2005). Phosphorylation-induced autoinhibition regulates the cytoskeletal protein Lethal (2) giant larvae. *Curr. Biol.* **15**, 276-282.

Blankenship, J. T., Backovic, S. T., Sanny, J. S., Weitz, O. and Zallen, J. A. (2006). Multicellular rosette formation links planar cell polarity to tissue morphogenesis. *Dev. Cell* **11**, 459-470.

Brown, K. E., Baonza, A. and Freeman, M. (2006). Epithelial cell adhesion in the developing Drosophila retina is regulated by Atonal and the EGF receptor pathway. *Dev. Biol.* **300**, 710-721.

Cooper, M. S., D'Amico, L. A. and Henry, C. A. (1999). Confocal microscopic analysis of morphogenetic movements. *Methods Cell Biol.* **59**, 179-204.

Cui, S., Otten, C., Rohr, S., Abdelilah-Seyfried, S. and Link, B. A. (2007). Analysis of aPKClambda and aPKCzeta reveals multiple and redundant functions during vertebrate retinogenesis. *Mol. Cell. Neurosci.* **34**, 431-444.

Dambly-Chaudière, C., Cubedo, N. and Ghysen, A. (2007). Control of cell migration in the development of the posterior lateral line: antagonistic interactions between the chemokine receptors CXCR4 and CXCR7/RDC1. *BMC Dev. Biol.* **29**, 7-23.

David, N. B., Sapède, D., Saint-Etienne, L., Thisse, C., Thisse, B., Dambly-Chaudière, C., Rosa, F. and Ghysen, A. (2002). Molecular basis of cell migration in the fish lateral line: Role of the chemokine receptor CXCR4 and of its ligand, SDF1. *Proc. Natl. Acad. Sci. USA* **99**, 16297-16302.

Dollar, G. L., Weber, U., Mlodzik, M. and Sokol, S. Y. (2005). Regulation of Lethal giant larvae by Dishevelled. *Nature* **437**, 1376-1380.

Ghysen, A. and Dambly-Chaudière, C. (2004). Development of the zebrafish lateral line. *Curr. Opin. Neurobiol.* **14**, 67-73.

Ghysen, A. and Dambly-Chaudière, C. (2007). The lateral line microcosmos. *Genes Dev.* **21**, 2118-2130.

Gompel, N., Cubedo, N., Thisse, C., Thisse, B., Dambly-Chaudière, C. and Ghysen, A. (2001). Pattern formation in the lateral line of the zebrafish. *Mech. Dev.* **105**, 69-77.

Haas, P. and Gilmour, D. (2006). Chemokine signaling mediates self-organizing tissue migration in the zebrafish lateral line. *Dev. Cell* **10**, 673-680.

Haines, L., Neyt, C., Gautier, P., Keenan, D. G., Bryson-Richardson, R. J., Hollway, G. E., Cole, N. J. and Currie, P. D. (2004). Met and Hgf signaling controls hypaxial muscle and lateral line development in the zebrafish. *Development* **131**, 4857-4869.

Horne-Badovinac, S., Lin, D., Waldron, S., Schwarz, M., Mbamalu, G., Pawson, T., Jan, Y., Stainier, D. Y. and Abdelilah-Seyfried, S. (2001). Positional cloning of *heart and soul* reveals multiple roles for PKC lambda in zebrafish organogenesis. *Curr. Biol.* **11**, 1492-1502.

Horne-Badovinac, S., Rebagliati, M. and Stainier, D. Y. (2003). A cellular framework for gut-looping morphogenesis in zebrafish. *Science* **302**, 662-665.

Itoh, M. and Chitnis, A. B. (2001). Expression of proneural and neurogenic genes in the zebrafish lateral line primordium correlates with selection of hair cell fate in neuromasts. *Mech. Dev.* **102**, 263-266.

Itoh, M., Kim, C. H., Palardy, G., Oda, T., Jiang, Y. J., Maust, D., Yeo, S. Y., Lorick, K., Wright, G. J., Ariza-McNaughton, L. et al. (2003). Mind bomb is a ubiquitin ligase that is essential for efficient activation of Notch signaling by Delta. *Dev. Cell* **4**, 67-82.

Jowett, T. and Lettice, L. (1994). Whole-mount in situ hybridization on zebrafish embryos using a mixture of digoxingenin- and fluorescin-labelled probes. *Trends Genet.* **10**, 73-74.

Kerstetter, A. E., Azodi, E., Marrs, J. A. and Liu, Q. (2004). Cadherin-2 function in the cranial ganglia and lateral line system of developing zebrafish. *Dev. Dyn.* **230**, 137-143.

Kimmel, C. B., Ballard, W. W., Kimmel, S. R., Ullmann, B. and Schilling, T. F. (1995). Stages of embryonic-development of the zebrafish. *Dev. Dyn.* **203**, 253-310.

Koester, R. W. and Fraser, S. E. (2001). Tracing transgene expression in living zebrafish embryos. *Dev. Biol.* **233**, 329-346.

Kollmar, R., Nakamura, S. K., Kappler, J. A. and Hudspeth, A. J. (2001). Expression and phylogeny of claudins in vertebrate primordia. *Proc. Natl. Acad. Sci. USA* **98**, 10196-10201.

Kozlowski, D. J., Whitfield, T. T., Hukriede, N. A., Lam, W. K. and Weinberg, E. S. (2005). The zebrafish dog-eared mutation disrupts eya1, a gene required for cell survival and differentiation in the inner ear and lateral line. *Dev. Biol.* **277**, 27-41.

Langheinrich, U., Hennen, E., Stott, G. and Vacun, G. (2002). Zebrafish as a model organism for the identification and characterization of drugs and genes affecting p53 signaling. *Curr. Biol.* **12**, 2023-2028.

Lecaudey, V., Cakan-Akdogan, G., Norton, W. H. and Gilmour, D. (2008). Dynamic Fgf signaling couples morphogenesis and migration in the zebrafish lateral line primordium. *Development* **135**, 2695-2705.

Liu, Q., Kerstetter, A. E., Azodi, E. and Marrs, J. A. (2003). Cadherin-1, -2, and -11 expression and cadherin-2 function in the pectoral limb bud and fin of the developing zebrafish. *Dev. Dyn.* **228**, 734-739.

López-Schier, H., Starr, C. J., Kappler, J. A., Kollmar, R. and Hudspeth, A. J. (2004). Directional cell migration establishes the axes of planar polarity in the posterior lateral-line organ of the zebrafish. *Dev. Cell.* **7**, 401-412.

Nasevicius, A. and Ekker, S. C. (2000). Effective targeted gene 'knockdown' in zebrafish. *Nat. Genet.* **26**, 216-220.

Nechiporuk, A. and Raible, D. W. (2008). FGF-dependent mechanosensory organ patterning in zebrafish. *Science* **320**, 1774-1777.

Peterson, R. T., Mably, J. D., Chen, J. N. and Fishman, M. C. (2001). Convergence of distinct pathways to heart patterning revealed by the small molecule concentramide and the mutation *heart-and-soul*. *Curr. Biol.* **11**, 1481-1491.

Plant, P. J., Fawcett, J. P., Lin, D. C., Holdorf, A. D., Binns, K., Kulkarni, S. and Pawson, T. (2003). A polarity complex of mPar-6 and atypical PKC binds, phosphorylates and regulates mammalian Lgl. *Nat. Cell Biol.* **5**, 301-308.

Robu, M. E., Larson, J. D., Nasevicius, A., Beiraghi, S., Brenner, C., Farber, S. A. and Ekker, S. C. (2007). p53 activation by knockdown technologies. *PLoS Genet.* **3**, e78.

Rohr, S., Bit-Avragim, N. and Abdelilah-Seyfried, S. (2006). Heart and soul/PRKCi and nagie oko/Mpp5 regulate myocardial coherence and remodeling during cardiac morphogenesis. *Development* **133**, 107-115.

Sahly, I., Andermann, P. and Petit, C. (1999). The zebrafish *eya1* gene and its expression pattern during embryogenesis. *Dev. Genes Evol.* **209**, 399-410.

Sarrazin, A. F., Villablanca, E. J., Nuñez, V. A., Sandoval, P. C., Ghysen, A. and Allende, M. L. (2006). Proneural gene requirement for hair cell differentiation in the zebrafish lateral line. *Dev. Biol.* **295**, 534-545.

Schlosser, G. (2006). Induction and specification of cranial placodes. *Dev. Biol.* **294**, 303-351.

Sonawane, M., Carpio, Y., Geisler, R., Schwarz, H., Maischein, H. M. and Nuesslein-Volhard, C. (2005). Zebrafish *penner/lethal giant larvae 2* functions in hemidesmosome formation, maintenance of cellular morphology and growth regulation in the developing basal epidermis. *Development* **132**, 3255-3265.

Valentin, G., Haas, P. and Gilmour, D. (2007). The chemokine SDF1a coordinates tissue migration through the spatially restricted activation of Cxcr7 and Cxcr4b. *Curr. Biol.* **17**, 1026-1031.

Westerfield, M. (1994). *The Zebrafish Book* (ed. M. Westerfield). Oregon: University of Oregon Press.

Wilson, A. L., Shen, Y. C., Babb-Clendenon, S. G., Rostedt, J., Liu, B., Barald, K. F., Marrs, J. A. and Liu, Q. (2007). Cadherin-4 plays a role in the development of zebrafish cranial ganglia and lateral line system. *Dev. Dyn.* **236**, 893-902.

Wolff, T. and Ready, D. F. (1993). Pattern formation in the *Drosophila* retina. In *The Development of* Drosophila melanogaster (ed. M. Bate and A. Martinez-Arias). Cold Spring Harbor, NY: Cold Spring Harbor Press.

Yamanaka, T., Horikoshi, Y., Sugiyama, Y., Ishiyama, C., Suzuki, A., Hirose, T., Iwamatsu, A., Shinohara, A. and Ohno, S. (2003). Mammalian Lgl forms a protein complex with PAR-6 and aPKC independently of PAR-3 to regulate epithelial cell polarity. *Curr. Biol.* **13**, 734-743.

Journal of Cell Science